

**FABRICATION AND CHARACTERIZATION OF GUM  
ARABIC BONDED *Rhizophora* spp. PARTICLEBOARD  
HEAD PHANTOM FOR PET/CT APPLICATIONS**

**By**

**ALI MOHAMMAD HAMDAN ABUARRA**

**Thesis submitted in fulfilment of the requirements  
for the degree of Doctor of Philosophy**

**Universiti Sains Malaysia**

**August 2014**

## **ACKNOWLEDGEMENT**

The submission of this thesis gives me an opportunity to express all praises to Allah, the almighty, merciful and passionate, for granting me the strengths to complete this thesis.

I highly show my regards to my main supervisor Assoc. Prof. Dr. Sabar Bauk for his great support, guidance in completion of my research work and patiently correcting my writing. I attribute the level of my PhD degree to his great help and encouragement. One simply could not wish for a better or friendlier supervisor.

I would also like to express my great thanks to my co-supervisor, Professor Rokiah Hashim, for her excellent guidance, caring, patience, and providing me with an excellent atmosphere for doing my research. She is really very expert in her field and has directed me through various situations, allowing me to reach this accomplishment. To her, I am eternally grateful.

Besides, I would like to thank my second co-supervisor, Associate Prof. Dr. Sivamany Kandaya for the continuous support of my PhD study and research. Her guidance insightful comments and suggestions helped me in all the time of research and writing of this thesis.

Special thanks go to the supporting staff of the laboratories in School of Physics, Archaeology centre, and School of Industry who helped me in many different ways to conduct the experiments in a specific manner.

I am also grateful to the people who helped and contribute great ideas and advices, especially my close friends: Dr. Ehsan Tousi, Dr. Saleh Ashrah, Dr. Mohamad wasef, Dr. Khaled Aldroobi, Dr. Eid Mahmoud, Mr. Amer Aljarah, Mr. Yahya Abbas, Mr. Zedan Alsade, Mr. Basher Abour and Mr. Baker Ababneh. Without them, this study would not be possible.

Great thanks to Universiti Sains Malaysia for the financial support of my Doctorate research by offering me a research grant 1001/pfizik/846085, to Penang Adventist Hospital, Malaysia, for permission to use their PET/CT facility. I would also like to thank the staff in Penang Pantai Hospital, Malaysia for the technical assistance in the calibration work. I highly appreciate their kind assistance.

Special thanks go to my parents, brothers and sisters, who have been the pillars behind the completion of my research by giving moral support and prayers. This work would never have been the light of the day: had it not been my parents. I am profoundly grateful to my parents.

I would additionally like to extend the deepest gratitude to my dear wife (Basma Abuarra) and lovely kids (Fatima, Zaina, Mohammad, and Aya) who were always there cheering me up and standing by me through the good times and bad. They were always supporting me and encouraging me with their best wishes.

Finally, I offer my regards and blessings to all of those who supported me in any respect during the completion of the research, as well as expressing my apology that I could not mention personally one by one.

Ali Abuarra, August 2014

## TABLE OF CONTENTS

|  | Page |
|--|------|
| <b>ACKNOWLEDGEMENT</b>                       | ii   |
| <b>TABLE OF CONTENTS</b>                     | iv   |
| <b>LIST OF TABLES</b>                        | x    |
| <b>LIST OF FIGURES</b>                       | xiv  |
| <b>LIST OF ABBREVIATIONS AND SYMBOLS</b>     | xx   |
| <b>ABSTRAK</b>                               | xxiv |
| <b>ABSTRACT</b>                              | xxvi |
| <b>CHAPTER ONE: INTRODUCTION</b>             | 1    |
| 1.1 Introduction                             | 1    |
| 1.2 Problem Statement                        | 6    |
| 1.3 Research significance                    | 7    |
| 1.4 Research Objectives                      | 8    |
| 1.5 Scope of Research                        | 8    |
| 1.6 Thesis Organization                      | 9    |
| <b>CHAPTER TWO: LITERATURE REVIEW</b>        | 10   |
| 2.1 <i>Rhizophora</i> spp. tree              | 10   |
| 2.2 Gum Arabic                               | 11   |
| 2.2.1 Chemical characteristics of gum Arabic | 13   |
| 2.2.2 Uses of gum Arabic                     | 15   |
| 2.2.3 Gum Arabic in food products            | 15   |

|  |   |    |
|--|---|----|
| 2.2.4  | Medical and pharmaceutical applications of gum Arabic     | 16 |
| 2.2.5  | Industrial applications of gum Arabic                     | 17 |
| 2.2.6  | Gum Arabic as a natural adhesive                          | 18 |
| 2.3  | X-ray fluorescence (XRF)                                  | 21 |
| 2.4  | Positron emission tomography/computed tomography (PET/CT) | 24 |
| 2.4.1  | Positron emission tomography (PET)                        | 25 |
| 2.4.2  | Computed tomography (CT)                                  | 27 |
| 2.4.3  | PET radiopharmaceutical tracers                           | 28 |
| 2.4.4  | Commercially available PET/CT phantoms                    | 29 |
| 2.5  | Thermoluminescent dosimetry (TLD)                         | 30 |
| 2.6  | Radiochromic film   | 33 |
| 2.7  | Review of <i>Rhizophora</i> spp. as phantom material      | 36 |
| 2.7.1  | <i>Rhizophora</i> spp. raw wood as phantom material       | 36 |
| 2.7.2  | <i>Rhizophora</i> spp. particleboard as phantom material  | 38 |
| <b>CHAPTER THREE: CHARACTERIZATION OF THE<br/>FABRICATED GUM ARABIC BONDED <i>Rhizophora</i> spp.<br/>PARTICLEBOARDS</b> |   | 45 |
| 3.1  | Introduction  | 45 |
| 3.2  | Materials and Methods                                     | 47 |
| 3.2.1  | Samples preparation                                       | 47 |
| 3.2.1.1  | Gum Arabic preparation                                    | 47 |
| 3.2.1.2  | <i>Rhizophora</i> spp. particles preparation              | 47 |
| 3.2.1.3  | Determination of the moisture content                     | 48 |

|         |  |    |
|---------|--|----|
| 3.2.1.4 | <i>Rhizophora</i> spp. particleboard fabrication   | 49 |
| 3.2.2   | Testing of the fabricated particleboards   | 52 |
| 3.2.2.1 | Measurement of gum Arabic and <i>Rhizophora</i> spp. particleboard densities by using gravimetric method | 52 |
| 3.2.2.2 | Measurement of the density by using CT scan  | 53 |
| 3.2.2.3 | Water absorption and thickness swelling tests  | 56 |
| 3.2.2.4 | Internal bond strength evaluation  | 57 |
| 3.2.2.5 | Microstrucure analysis by FE-SEM   | 57 |
| 3.2.2.6 | Determination of the linear and mass attenuation coefficients of particleboard samples                   | 58 |
| 3.2.2.7 | Analysis of the CHNS elemental composition   | 63 |
| 3.2.2.8 | Evaluation of the effective atomic number $Z_{eff}$  | 64 |
| 3.3     | Results and discussion   | 66 |
| 3.3.1   | Analysis of the moisture content   | 66 |
| 3.3.2   | Density measurement by using gravimetric method  | 67 |
| 3.3.3   | Density measurement by using CT scan   | 68 |
| 3.3.4   | Evaluation of the thickness swelling (TS) and water absorption (WA)                                      | 73 |
| 3.3.5   | Evaluation of internal bond strength   | 77 |
| 3.3.6   | Microstrucure analysis by FE-SEM   | 79 |
| 3.3.7   | The mass attenuation coefficients of <i>Rhizophora</i> spp.  | 82 |
| 3.3.8   | CHNS Analysis  | 89 |
| 3.3.9   | Effective atomic number ( $Z_{eff}$ ) evaluation   | 92 |

|     |            |    |
|-----|------------|----|
| 3.4 | Conclusion | 93 |
|-----|------------|----|

## **CHAPTER FOUR: DESIGN, FABRICATION AND APPLICATION OF THE FABRICATED GUM ARABIC BONDED *Rhizophora* spp. PARTICLEBOARD HEAD PHANTOMS IN PET/CT IMAGING**

|         |   |     |
|---------|---|-----|
| 4.1     | Introduction  | 95  |
| 4.2     | Materials and Methods   | 97  |
| 4.2.1   | Phantoms' preparation   | 97  |
| 4.2.1.1 | GA bonded <i>Rhizophora</i> spp. particleboard phantom        | 98  |
| 4.2.1.2 | Water phantom design  | 99  |
| 4.2.1.3 | Perspex phantom design  | 100 |
| 4.2.2   | Dosimetric preparation  | 101 |
| 4.2.2.1 | Preparation of thermoluminescent dosimeters                   | 101 |
| a.      | Annealing of TLDs   | 102 |
| b.      | Irradiation of the TLDs                                       | 102 |
| c.      | TLD read out  | 103 |
| d.      | Relative sensitivity and sensitivity factor of TLDs           | 103 |
| e.      | Calibration and dose response of TLD-100                      | 105 |
| 4.2.2.2 | Gafchromic XR- QA2 film                                       | 105 |
| 4.2.3   | PET/CT scan   | 108 |
| 4.2.3.1 | Phantom preparations for PET/CT scan                          | 108 |
| 4.2.3.2 | Image acquisition   | 111 |
| 4.2.4   | Measurement of the CT numbers of the fabricated head phantoms | 112 |

|             |  |     |
|-------------|--|-----|
| 4.2.5       | Measurement of the skin surface dose                         | 113 |
| 4.3         | Results and discussion                                       | 114 |
| 4.3.1       | Screening of TLD-100   | 114 |
| 4.3.2       | Calibration curves of TLD-100 and Gafchromic film XR- QA2    | 118 |
| 4.3.3       | PET/CT scan  | 119 |
| 4.3.4       | Measurement of the fabricated head phantoms' CT numbers      | 130 |
| 4.3.5       | Skin surface dose measurement                                | 132 |
| 4.3.5.1     | Skin surface dose measurement by TLD-100                     | 133 |
| 4.3.5.2     | Skin surface dose measurement by Gafchromic XR- QA2 film     | 135 |
| 4.3.5.3     | Effect of detector distance from the tumor simulating sphere | 138 |
| 4.4         | Conclusion   | 145 |
|             | <b>CHAPTER FIVE: CONCLUSIONS AND FUTURE WORK</b>             | 147 |
| 5.1         | Conclusions  | 147 |
| 5.2         | Recommendations for future work                              | 150 |
|             | <b>REFERENCES</b>  | 152 |
|             | <b>APPENDICES</b>  | 164 |
| Appendix A: | Data for thickness swelling and water absorption tests       | 164 |
| Appendix B: | Data of the linear attenuation coefficients                  | 165 |



|   |     |
|---|-----|
| Appendix C: Data for the five screening cycles of a batch of 224 TLD-100 chips      | 175 |
| Appendix D: Data for skin surface dose measurements in the fabricated head phantoms | 203 |
| <b>LIST OF PUBLICATIONS</b>   | 215 |

## LIST OF TABLES

|           |  |    |
|-----------|--|----|
| Table 2.1 | Chemical composition and some properties of <i>Acacia senegal</i> gum.   | 14 |
| Table 2.2 | Summary of the literature on using <i>Rhizophora</i> spp wood as a phantom material.   | 41 |
| Table 3.1 | The identification codes of gum Arabic (GA) adhesive and the twelve fabricated <i>Rhizophora</i> spp. particleboard samples.   | 49 |
| Table 3.2 | Properties of the used metal plates and their $K\alpha_1$ fluorescence energies (keV) at energy range 17.4-26.7 keV.   | 60 |
| Table 3.3 | Data for the mass attenuation coefficient of particleboard sample A <sub>15</sub> .  | 62 |
| Table 3.4 | Summary of the manufactured <i>Rhizophora</i> spp. particleboard samples bonded with gum Arabic.   | 67 |
| Table 3.5 | Measured average CT numbers and densities calculated from CT numbers for the fabricated particleboard samples. Densities are expressed as mean value $\pm$ standard deviation.                         | 70 |
| Table 3.6 | Mass attenuation coefficients of aluminium measured at different XRF beam effective energies and compared with the XCOM calculated values.   | 82 |
| Table 3.7 | The measured linear and mass attenuation coefficients of <i>Rhizophora</i> spp. particleboard samples and the gum depending on the $K\alpha_1$ peaks of the characteristic X-ray of the metal targets. | 83 |
| Table 3.8 | Mass attenuation coefficients of <i>Rhizophora</i> spp. particleboards measured in XRF at different effective energies (keV) and the XCOM calculated mass attenuation coefficient of water.            | 84 |
| Table 3.9 | The <i>t</i> -test of the mass attenuation coefficient of <i>Rhizophora</i>  | 87 |

spp. particleboards compared to water.

|            |   |     |
|------------|---|-----|
| Table 3.10 | The elemental composition of <i>Rhizophora</i> spp. particles, gum Arabic and gum Arabic- <i>Rhizophora</i> spp. mixture.   | 90  |
| Table 3.11 | The elemental composition of some human organs, tissues and other tissue equivalent materials.  | 91  |
| Table 3.12 | The effective atomic number ( $Z_{eff}$ ) values for <i>Rhizophora</i> spp. (Rh), gum Arabic powder (GA), and gum Arabic bonded <i>Rhizophora</i> spp. (Rh5) particles.                                 | 93  |
| Table 4.1  | The CT numbers of the three fabricated cylindrical head phantoms: Gum Arabic bonded <i>Rhizophora</i> spp. particleboard, Perspex, and water phantoms, respectively.                                    | 130 |
| Table 4.2  | The measured skin surface dose (cGy) of the fabricated gum Arabic bonded <i>Rhizophora</i> spp. particleboard (Rh), Perspex and water head phantoms by using Harshaw TLD-100 chips after PET/CT scan.   | 134 |
| Table 4.3  | The measured skin surface dose (cGy) of the fabricated gum Arabic bonded <i>Rhizophora</i> spp. particleboard (Rh), Perspex and water head phantoms by using Gafchromic XR- QA2 film after PET/CT scan. | 136 |
| Table 4.4  | The skin surface dose from the TLD-100 located in the same ring level in the Perspex phantom.   | 140 |
| Table 4.5  | The skin surface dose from the TLD-100 located in the same ring level in the fabricated gum Arabic bonded <i>Rhizophora</i> spp. particleboard phantom.   | 140 |
| Table 4.6  | The skin surface dose from the TLD-100 located in the same ring level in the water phantom.   | 141 |
| Table 4.7  | The skin surface dose from the Gafchromic XR- QA2 film located in the same ring level in the fabricated Perspex head phantom.   | 142 |
| Table 4.8  | The skin surface dose from the Gafchromic XR- QA2 film located in the same ring level in the fabricated gum Arabic bonded <i>Rhizophora</i> spp. particleboard phantom.                                 | 142 |

|            |   |     |
|------------|---|-----|
| Table 4.9  | The skin surface dose from the Gafchromic XR- QA2 film located in the same ring level in the fabricated water head phantom.   | 143 |
| Table A. 1 | Data for thickness swelling (%) of the <i>Rhizophora</i> spp. particleboard samples.  | 164 |
| Table A. 2 | Data for water absorption (%) of the <i>Rhizophora</i> spp. particleboard samples.  | 164 |
| Table B. 1 | The linear attenuation coefficients of the fabricated gum Arabic bonded <i>Rhizophora</i> spp. particleboard samples at 17.4 keV energy from Niobium (Nb) plate.    | 165 |
| Table B. 2 | The linear attenuation coefficients of the fabricated gum Arabic bonded <i>Rhizophora</i> spp. particleboard samples at 18.5 keV energy from Molybdenum (Mo) plate. | 167 |
| Table B. 3 | The linear attenuation coefficients of the fabricated gum Arabic bonded <i>Rhizophora</i> spp. particleboard samples at 22.4 keV energy from Palladium (Pd) plate.  | 169 |
| Table B. 4 | The linear attenuation coefficients of the fabricated gum Arabic bonded <i>Rhizophora</i> spp. particleboard samples at 23.5 keV energy from silver (Ag) plate.     | 171 |
| Table B. 5 | The linear attenuation coefficients of the fabricated gum Arabic bonded <i>Rhizophora</i> spp. particleboard samples at 26.7 keV energy from Tin (Sn) plate.        | 173 |
| Table C. 1 | The TLD reading for five screening cycles (C).  | 175 |
| Table C. 2 | The relative sensitivity of TLD-100 for five screening cycles.  | 184 |
| Table C. 3 | The sensitivity factor of TLD-100 for five screening cycles.  | 193 |
| Table C.4  | Data for the calibration of TLD-100 and Gafchromic XR-QA2 film.   | 202 |
| Table D. 1 | Skin surface dose measurements in the fabricated gum Arabic   | 203 |

bonded *Rhizophora* spp. particleboard head phantom by using TLD-100 chips.

|            |  |     |
|------------|--|-----|
| Table D. 2 | Skin surface dose measurements in the fabricated perspex head phantom by using TLD-100 chips.  | 205 |
| Table D. 3 | Skin surface dose measurements in the fabricated water head phantom by using TLD-100 chips.  | 207 |
| Table D. 4 | Skin surface dose measurements in the fabricated gum Arabic bonded <i>Rhizophora</i> spp. particleboard head phantom by using Gafchromic film XR- QA2. | 209 |
| Table D. 5 | Skin surface dose measurements in the fabricated perspex head phantom by using Gafchromic film XR- QA2.  | 211 |
| Table D. 6 | Skin surface dose measurements in the fabricated water head phantom by using Gafchromic film XR- QA2.  | 213 |

## LIST OF FIGURES

|          |  |    |
|----------|--|----|
| Fig. 2.1 | The mangrove <i>Rhizophora</i> spp. trees (Larut Matang) from a forest reserve in Perak, Malaysia.   | 10 |
| Fig. 2.2 | Gum Arabic flowing from the bark of <i>Acacia senegal</i> tree (Cecil, 2005).  | 13 |
| Fig. 2.3 | Principle of XRF radiation. Incident X-rays extract a K level electron. Either $K_{\alpha}$ or $K_{\beta}$ radiation is emitted, depending on whether the vacancy in the K shell is filled by an L or M electron (Riise et al., 2000). | 22 |
| Fig. 2.4 | The production of two annihilation photons from the collision of an electron and a positron emitted from a radioactive isotope (Schmitz et al., 2005).   | 26 |
| Fig. 2.5 | Schematic diagram showing the main components of combined PET/CT scanner (Schmitz et al., 2005).   | 27 |
| Fig. 2.6 | A commercially available PET/CT phantom with the internal inserts of three rods and six spheres (Biodex, 2014).  | 29 |
| Fig. 2.7 | Illustration of thermoluminescence process. The ionizing radiation triggers the electrons and the holes to migrate and get trapped; while the addition of heat releases the electrons and photons are produced (Attix, 2008).          | 31 |
| Fig. 3.1 | Gum Arabic from <i>Acacia</i> tree, (a) tears shape, (b) powder form.  | 47 |
| Fig. 3.2 | Automatic moisture analyzer (MAC 50/NH) used to measure the moisture content of GA powder and <i>Rhizophora</i> spp. particles.  | 49 |
| Fig. 3.3 | Preparation of the GA bonded <i>Rhizophora</i> spp. particleboard samples: a) <i>Rhizophora</i> spp. stems, b) <i>Rhizophora</i> spp. particles, c) GA- <i>Rhizophora</i> spp. mixture, d) GA bonded <i>Rhizophora</i> spp.            | 51 |

particleboard in stainless steel frame.

|           |   |    |
|-----------|---|----|
| Fig. 3.4  | Gum Arabic buttons used for gum density calculation with thicknesses of (a) 0.76 cm, (b) 0.58 cm, (c) 0.41 cm, and (d) 0.25 cm.   | 52 |
| Fig. 3.5  | Calibration curve of CT number versus density at 120 kVp.   | 55 |
| Fig. 3.6  | Instruments used to obtain the micrographs of GA and <i>Rhizophora</i> spp. particleboard samples, a) Quorum sputter coater, b) Field emission- scanning electron microscope.   | 58 |
| Fig. 3.7  | The experimental set up for the measurement of the linear attenuation coefficients of GA treated <i>Rhizophora</i> spp. particleboards using x-ray fluorescence (XRF) beam.   | 59 |
| Fig. 3.8  | Curve for calculating the mass attenuation coefficient of sample A <sub>15</sub> .  | 62 |
| Fig. 3.9  | Fully automated PerkinElmer 2400 Series II CHNS/O Elemental Analyzer used for the elemental composition analysis.   | 64 |
| Fig. 3.10 | The CT images acquired for the fabricated particleboard samples, water, air, and high purity aluminium plate. (a) Scout CT image for all the samples, (b) Scout CT image of all the samples with the scanning parameters and the CT number values of the two regions of interest (ROI), (c) Axial CT image of four particleboard samples, (d) Axial CT image of the aluminium plate, air and water (from left to right). The A, B, and C refer to the samples described in Table 3.1. | 68 |
| Fig. 3.11 | The density of the fabricated particleboard samples calculated from the CT number as compared to the density obtained from the gravimetric method.  | 71 |
| Fig. 3.12 | Thickness swelling (%) of the fabricated <i>Rhizophora</i> spp. particleboards. A, B, and C refer to the samples with particle sizes of 149 - 210 $\mu\text{m}$ , 74 - 149 $\mu\text{m}$ , and < 74 $\mu\text{m}$ respectively, while, 0, 5, 10 and 15 refer to the adhesive percentage in the particleboards.  | 73 |

|           |   |     |
|-----------|---|-----|
| Fig. 3.13 | Water absorption (%) of the fabricated <i>Rhizophora</i> spp. particleboards. A, B, and C refer to the samples with particle sizes of 149 - 210 $\mu\text{m}$ , 74 - 149 $\mu\text{m}$ , and < 74 $\mu\text{m}$ respectively, while, 0, 5, 10 and 15 refer to the adhesive percentage in the particleboards.                                    | 75  |
| Fig. 3.14 | Internal bond strength of <i>Rhizophora</i> spp. particleboards fabricated with and without gum Arabic binder. A, B, and C refer to the samples with particle sizes of 149 - 210 $\mu\text{m}$ , 74 - 149 $\mu\text{m}$ , and < 74 $\mu\text{m}$ respectively, while, 0, 5, 10 and 15 refer to the gum Arabic percentage in the particleboards. | 77  |
| Fig. 3.15 | Field Emission- Scanning Electron Micrographs (FE-SEM) of particleboards manufactured from <i>Rhizophora</i> spp. particles (74 - 149 $\mu\text{m}$ ) at 500 X. B <sub>0</sub> is the binderless particleboard, while, B <sub>5</sub> & B <sub>15</sub> are particleboard samples bonded with 5% and 15% of gum Arabic, respectively.           | 79  |
| Fig. 3.16 | Field Emission Scanning Electron Micrographs (FE-SEM) of particleboards fabricated from <i>Rhizophora</i> spp. stems (149 - 210 $\mu\text{m}$ ) at 3000 X. B <sub>0</sub> is the binderless particleboard, while, B <sub>5</sub> & B <sub>15</sub> are particleboard samples bonded with 5% and 15% of gum Arabic, respectively.                | 81  |
| Fig. 3.17 | Mass attenuation coefficients of <i>Rhizophora</i> spp. particleboards from the counts under the K <sub><math>\alpha</math>1</sub> XRF peaks of the different samples as compared with water (calculated in XCOM).  | 85  |
| Fig. 4.1  | The three types of cylindrical head phantoms that were fabricated in this study. a) Water phantom, b) gum Arabic bonded <i>Rhizophora</i> spp. particleboard phantom, and c) Perspex phantom.   | 98  |
| Fig. 4.2  | The fabricated gum Arabic bonded <i>Rhizophora</i> spp. particleboard cylindrical head phantom for PET/CT applications. The bottom of the phantom with the four plastic rods and screws are shown at the right.   | 99  |
| Fig. 4.3  | The geometric design and the fabricated water head phantom with the tumour representing sphere held at 5 cm from top.   | 100 |



|           |  |     |
|-----------|--|-----|
| Fig. 4.4  | The fabricated cylindrical Perspex head phantom with the tumour representing sphere drilled at 5 cm from top.  | 101 |
| Fig. 4.5  | The marked locations for TLDs and films on the surface of the three fabricated head phantoms: a) Gum Arabic bonded <i>Rhizophora</i> spp. particleboard head phantom, b) Perspex head phantom, c) water head phantom, d) Illustration of the dosimeters' distribution on the phantoms' surfaces and e) Perspex head phantom with the TLD-100 chips and Gafchromic XR- QA2 films (orange colour) distributed on the phantom's surface and fixed by adhesive tape (blue colour). | 109 |
| Fig. 4.6  | Schematic diagram of the control dosimeters used with each phantom. The TLD chips and Gafchromic XR- QA2 film piece were placed at 1 cm distance from each others.   | 110 |
| Fig. 4.7  | The designed cylindrical water head phantom, (a) the position and orientation of the phantom on the examination table, (b) the alignment with laser beam.  | 111 |
| Fig. 4.8  | The relative sensitivity of TLD-100 chips for five screening cycles.   | 115 |
| Fig. 4.9  | The sensitivity factor of TLD-100 chips for five screening cycles.   | 116 |
| Fig. 4.10 | Dose calibration curve of TLD-100 at 6 MV linear accelerator (LINAC).  | 118 |
| Fig. 4.11 | Calibration curve of absorbed dose versus the optical for Gafchromic XR- QA2.  | 119 |
| Fig. 4.12 | PET/CT images of the fabricated gum Arabic bonded <i>Rhizophora</i> spp. particleboard cylindrical head phantom: a) scout CT scan, b) axial CT slice of a region without tumour, c) axial CT slice showing the simulated tumour as bright circle near the centre, d) non attenuated corrected PET image, e) PET image whose attenuation was corrected using CT data, f) axial view of fused PET/CT image without tumour, g) axial view of                                      | 120 |

fused PET/CT image with simulated tumour appeared as red circle near the centre, h) coronal view of fused PET/CT image with simulated tumour appeared in the upper part of the phantom, i) the line spacing used for locating the simulated tumour site.

- Fig. 4.13 PET/CT images of the fabricated cylindrical perspex head phantom: a) scout CT scan, b) axial CT slice of a region without tumour, c) axial CT slice showing the simulated tumour as bright circle near the centre, d) non attenuated corrected PET image, e) PET image whose attenuation was corrected using the CT data, f) axial view of fused PET/CT image without tumour, g) axial view of fused PET/CT image with simulated tumour appeared as red circle near the centre, h) coronal view of fused PET/CT image with simulated tumour appeared in the upper part of the phantom, i) the line spacing used for locating the simulated tumour site. 125
- Fig. 4.14 PET/CT images of the fabricated cylindrical water head phantom: a) scout CT scan, b) axial CT slice of a region without tumour, c) axial CT slice showing the simulated tumour as bright circle near the centre, d) non attenuated corrected PET image, e) PET image whose attenuation was corrected using the CT data, f) axial view of fused PET/CT image without tumour, g) axial view of fused PET/CT image with simulated tumour appeared as red circle near the centre, h) coronal view of fused PET/CT image with simulated tumour appeared in the upper part of the phantom, i) the line spacing used for locating the simulated tumour site. 127
- Fig. 4.15 CT image of fabricated head phantoms made of *Rhizophora* spp. a) Raw wood (Omar, 2007), and b) Particleboards. Intact structure, uniform density distribution and absence of deformities are the distinct characteristics of the fabricated particleboard over the raw wood phantoms. 129
- Fig. 4.16 A graphic representation of different structures on CT with their relative HU values (Kennedy, 2014). 131
- Fig. 4.17 The HU greyscale in correlation to air, water and some human tissues (Jerke, 2012). 131

|           |   |     |
|-----------|---|-----|
| Fig. 4.18 | The location of the tumour simulating sphere in the three fabricated head phantoms with the relative distances (in units) from the phantoms borders.  | 138 |
| Fig. 4.19 | The arrangement of the TLD-100 chips on the surface of the fabricated phantoms. Each phantom had 5 rings and each ring had twelve TLD chips.  | 139 |
| Fig. 4.20 | Mapping of the skin surface dose measurements in the fabricated gum Arabic bonded <i>Rhizophora</i> spp. particleboard phantom by using the <i>Kriging</i> method. The measurements were obtained from the TLD-100 and Gafchromic XR- QA2 film. | 144 |
| Fig. 4.21 | Mapping of the skin surface dose measurements in the fabricated perspex head phantom by using the <i>Kriging</i> method. The measurements were obtained from the TLD-100 and Gafchromic XR- QA2 film.   | 144 |
| Fig. 4.22 | Mapping of the skin surface dose measurements in the fabricated water head phantom by using the <i>Kriging</i> method. The measurements were obtained from the TLD-100 and Gafchromic XR- QA2 film.   | 145 |

## LIST OF ABBREVIATIONS AND SYMBOLS

|                      |  |
|----------------------|--|
| AC                   | Attenuation Correction                         |
| Av                   | Average  |
| BC                   | Before Christ                                  |
| $^{11}\text{C}$      | Carbon-11                                      |
| CF                   | Calibration Factor                             |
| cGy                  | Centigray                                      |
| CHNS                 | Carbon Hydrogen Nitrogen Sulfur                |
| Co-60                | Cobalt-60                                      |
| Cs-137               | Caesium-137                                    |
| CT                   | Computed Tomography                            |
| CTAC                 | Computed Tomography Attenuation Correction     |
| DICOM                | Digital Imaging and Communications in Medicine |
| $D_{\text{max}}$     | Maximum depth                                  |
| Dpi                  | Dot per inch                                   |
| ECC                  | Element Correction Coefficient                 |
| $^{18}\text{F}$ -FDG | $^{18}\text{F}$ -fluorodeoxyglucose            |
| FE-SEM               | Field emission-scanning electron microscopy    |
| FWHM                 | Full Width at Half Maximum                     |
| GA                   | Gum Arabic                                     |
| GE                   | General Electric                               |
| LEGe                 | Low Energy Germanium                           |

|                   |   |
|-------------------|---|
| Gy                | Gray  |
| HU                | Hounsfield Units                                    |
| $I$               | Intensity of attenuated narrow beam of gamma-ray    |
| <i>i.e.</i>       | That is   |
| $I_0$             | Intensity of un-attenuated narrow beam of gamma-ray |
| IAEA              | International Atomic Energy Agency                  |
| IB                | Internal Bond                                       |
| Ir-192            | Iridium-192   |
| JIS               | Japanese Industrial Standards                       |
| keV               | Kilo electron volt                                  |
| kV                | Kilovolt  |
| kVp               | Peak kilovoltage                                    |
| LINAC             | Linear accelerator                                  |
| m/v               | Mass by Volume                                      |
| mA                | Miliampere  |
| mAs               | milliampere-second                                  |
| MC                | Moisture Content                                    |
| MeV               | Mega electron volt                                  |
| MOE               | Modulus of Elasticity                               |
| MOR               | Modulus of Rupture                                  |
| MPa               | Megapascal  |
| mR                | Milli Rontengen                                     |
| N/mm <sup>2</sup> | Newton per square millimetre                        |

|                 |  |
|-----------------|--|
| nC              | Nanocoulomb                                      |
| °C              | Degree Celsius                                   |
| OD              | Optical Density                                  |
| PET             | Positron Emission Tomography                     |
| PET/CT          | Positron Emission Tomography/Computed Tomography |
| PF              | phenol-formaldehyde                              |
| PMT             | Photomultiplier tube                             |
| PV              | Pixel value                                      |
| QC              | Quality control                                  |
| R               | Rontengen  |
| ROI             | Region of interest                               |
| SO <sub>2</sub> | Sulfur dioxide                                   |
| SPECT           | Single-photon emission computed tomography       |
| spp             | Species  |
| SSD             | Source-to-sample distance                        |
| STD             | Standard Deviation                               |
| TL              | Thermoluminescence                               |
| TLD             | Thermoluminescence dosimeter                     |
| TS              | Thickness swelling                               |
| TTP             | Time temperature profile                         |
| UF              | Urea formaldehyde                                |
| UV              | Ultra violet                                     |
| w/w             | Weight by weight                                 |

|                  |                                |
|------------------|--------------------------------|
| WA               | Water absorption               |
| X                | Magnification                  |
| XCOM             | X-ray computed                 |
| XRF              | X-ray fluorescence             |
| Z                | Atomic number                  |
| $Z_{\text{eff}}$ | Effective atomic number        |
| $\alpha$         | Alpha                          |
| $\beta$          | Beta                           |
| $\gamma$         | Gamma                          |
| $\mu$            | Linear attenuation coefficient |
| $\mu/\rho$       | Mass attenuation coefficient   |
| $\mu\text{Ci}$   | Microcurie                     |
| $\mu\text{Gy}$   | Microgray                      |
| $\rho$           | Density                        |

## **FABRIKASI DAN PENCIRIAN FANTOM KEPALA PAPAN SERPAI**

### ***Rhizophora* spp. BERIKAT GAM ARAB BAGI KEGUNAAN PET/CT**

#### **ABSTRAK**

Gam Arab telah ditambah ke dalam papan serpai *Rhizophora* spp. dengan tiga saiz zarah (149 - 210  $\mu\text{m}$ , 74 - 149  $\mu\text{m}$ , dan < 74  $\mu\text{m}$ ). Pada empat tahap perekat GA yang berbeza (0%, 5 %, 10 %, dan 15%). Ketumpatan, kandungan lembapan (MC), kekuatan ikatan dalaman (IB), bengkak ketebalan (TS), penyerapan air (WA), CHNS (karbon, hidrogen, nitrogen, dan sulfur), morfologi struktur dan peng ukuran pekali atenuasi tisu telah digunakan untuk mencirikan papan serpai yang dihasilkan.

Kemudian, sampel papan serpai dengan ciri-ciri terbaik telah digunakan untuk fabrikasi fantom kepala silinderan dengan saiz standard 16 cm diameter dan ketinggian 15 cm. Fantom kepala Perspek dan air juga telah dibuat dalam kajian ini dengan saiz dan bentuk yang sama seperti fantom papan serpai *Rhizophora* spp. Sifat-sifat dosimetri daripada fantom-fantom ini telah dinilai dalam PET/CT scan pada 511 keV. Fantom-fantom telah digunakan untuk mengukur dos permukaan kulit dengan menggunakan cip TLD -100 dan dosimeter filem Gafchromic XR- QA2.

Kajian menunjukkan bahawa penambahan GA ke dalam papan serpai nyata telah menambah baik sifat-sifat papan serpai secara keseluruhan. Imbasan PET/CT menunjukkan persetujuan baik antara data fantom kepala papan serpai *Rhizophora* spp. berbanding dengan fantom standard perspek dan air. Semua fantom kepala yang direka muncul dengan taburan skala kelabu yang sama dalam imej-imej CT yang menunjukkan ketumpatan yang seragam dan kandungan yang sekata.



Berdasarkan keputusan di atas, gam Arab didapati sebagai bio-perekat semulajadi yang berkesan yang boleh digunakan untuk pembuatan papan serpai dengan sifat-sifat yang lebih baik. Selain itu, sample papan serpai *Rhizophora* spp. mempunyai potensi yang baik bagi mewakili tisu manusia khususnya, tisu payudara manusia. Oleh itu, papan serpai terikat GA amat disyorkan untuk digunakan sebagai bahan fantom setaraan tisu hantu bersamaan untuk aplikasi dosimetri dalam PET/CT dan kawasan radiologi lain. Fantom papan serpai *Rhizophora* spp. terikat GA boleh direka dengan ciri-ciri dosimetri yang diinginkan dan kos yang minimum berbanding dengan fantom-fantom yang boleh didapati secara komersial.

**FABRICATION AND CHARACTERIZATION OF GUM ARABIC  
BONDED *Rhizophora* spp. PARTICLEBOARD HEAD PHANTOM FOR PET/CT  
APPLICATIONS**

**ABSTRACT**

Gum Arabic was used to manufacture *Rhizophora* spp. particleboards with three particle sizes (149 - 210  $\mu\text{m}$ , 74 - 149  $\mu\text{m}$ , and < 74  $\mu\text{m}$ ) at four different GA adhesive levels (0%, 5%, 10%, and 15%). The density, moisture content (MC), internal bond (IB) strength, thickness swelling (TS), water absorption (WA), CHNS (carbon, hydrogen, nitrogen, and sulfur), structural morphology and the mass attenuation coefficient measurements were used to characterize the fabricated particleboards.

The particleboard sample with the optimum properties was used for the fabrication of cylindrical head phantom with a standard size of 16 cm diameter and 15 cm height. Perspex and water head phantoms were also used in this study with the same size and shape as the *Rhizophora* spp. particleboard phantom. The dosimetric properties of the fabricated phantoms were evaluated in PET/CT scan at 511 keV. The phantoms were used to measure the skin surface dose by using TLD-100 chips and Gafchromic XR- QA2 film dosimeters.

The addition of GA into the particleboards improved the particleboard overall properties. The PET/CT scan indicated the good agreement between the data of the fabricated *Rhizophora* spp. particleboard head phantom compared to the standard perspex and water phantoms. The tumour simulating sphere was clearly seen and precisely localized in the PET/CT images of the three head phantoms. All the fabricated

head phantoms appeared with similar greyscale distribution in the CT images which indicated the uniform density and homogenous composition. The dose measurements of the three phantom materials indicated the approximate dosimetric abilities of gum Arabic bonded *Rhizophora* spp. particleboard as comparable to the standard perspex and water phantoms.

Based on the above results, gum Arabic was found to be an effective natural bio-adhesive that could be utilized to manufacture particleboards with improved properties. Besides, *Rhizophora* spp. particleboard samples have the potential to be good representatives of human tissues, specifically the human breast tissue. Therefore, GA bonded particleboards can be highly recommended to be used as tissue equivalent phantom material for dosimetric applications in PET/CT and other radiological areas. The gum Arabic bonded *Rhizophora* spp. particleboard phantom could be fabricated with favourable dosimetric properties and minimal cost compared to the commercially available phantoms.

## **CHAPTER ONE**

### **INTRODUCTION**

#### **1.1 Introduction**

Basically, the phantom is a tissue equivalent material used to simulate a real tissue of the patient by measuring the dose distribution in order to correlate the absorbed dose to the tissues (Yohannes et al., 2012). There are several commercially available tissue characterization phantoms that are designed to simulate certain parts of the human body, such as the head and the abdomen. The phantoms are composed of tissue substitute materials and contain holes that can accommodate inserts made from materials of known radiological properties. Water phantom is considered as the primary phantom recommended for dosimetry as water is the perfect match with tissue, but since it is not always practical to perform dosimetric measurements in liquid medium, solid homogeneous phantoms made from polystyrene, acrylic and other proprietary materials have become preferred substitute to water phantoms (Khan, 2010).

A material is regarded equivalent to a real tissue if it possesses the same radiation characteristics within the relevant energy range in addition to similar physical properties such as mass density and electron density. Currently, there are several commercially available tissue equivalent materials which offer simple, convenient and accurate simulations for therapy dose determinations in electron and photon applications. Tissue equivalent materials are widely used in routine quality assurance and quality control of diagnostic and therapeutic physics. In radiotherapy, they are usually used for

computed tomography (CT) number calibration in treatment planning systems. Moreover, they are frequently used to measure doses delivered to patients undergoing various therapeutic procedures. However, current available tissue equivalent materials may not be very accurate in the determination of the calibration curves because of their limitation in mimicking radiation characteristics of the corresponding real tissues in both low and high energy ranges encountered in diagnostic radiology (Yohannes et al., 2012). Therefore, it is necessary to look for new materials with tissue equivalent properties for the calibration purposes.

A few decades ago, efforts have been employed in the evaluation and characterization of photon attenuation for a wide range of materials (Hubbell et al., 1986). The mass attenuation coefficient of various elements and compounds of biological and dosimetric materials have been studied by some authors. Worth of notice are the efforts in characterizing photon attenuation for wood. For example, considerable research has been focused on the suitability of the mangrove hardwood *Rhizophora* spp. as tissue equivalent phantom material (Bradley et al., 1988; Bradley et al., 1991; Tajuddin et al., 1996; Abdel Munem, 1999; Rahman et al., 2000; Banjade, 2001; Bauk and Tajuddin 2008; Ibrahim, 2008; Shakhreet et al., 2009; Marashdeh et al., 2012; Safian, 2012; and Shakhreet et al., 2013).

*Rhizophora* is a genus of mangrove trees which can be found growing abundantly in the tropical and subtropical coastal regions. All *Rhizophora* species are closely similar in tree form and only specialists can differentiate them. Therefore, *Rhizophora* spp. will be used to indicate unidentified *Rhizophora* species. Currently, they are mainly used as firewood, timber, charcoal, construction material and dyes due

to the high tannin content of the bark of most *Rhizophora* spp. Moreover, the trees are also used for the lignocellulose for chipboard, pulpwood, newspaper and cardboard manufacture (Ng et al., 1999). In traditional medicine, they are used to treat angina, boils, leprosy, fever, malaria, diarrhoea, dysentery, and fungal infections (Duke and Allen, 2006).

According to previous reports, *Rhizophora* spp. wood has attenuation properties that match with water and breast tissue, but, it was found that the density of the raw wood was not uniform and the wood itself cracked after some time (Omar, 2007). He suggested for future work of grinding the raw wood into small particles and compressing them into particleboards might improve the attenuation properties, allow the addition of other extra substances that enhance the physical and mechanical properties of the particleboards and will facilitate the fabrication of tissue equivalent phantoms in the desired shape, density and size. Shakhreet (2006) was the first to fabricate the *Rhizophora* spp. wood into particleboards.

In general, a particleboard can be defined as a wood based composite that consists of cellulosic particles of various shape and sizes bonded together with an adhesive under heat and pressure (JIS, 2003). Particleboards can also be fabricated without using any adhesive and would be called binderless particleboards. The binding will be due to the presence of free sugars and lignocellulosic substances in the wood tissue where heat and pressure would cause them to be the binders within the particleboard. Although, binderless particleboards have preferable attenuation properties, they also have inferior internal bond strength and dimensional stability in the case of water absorption and thickness swelling (Marashdeh, 2013). On the other hand, the

addition of synthetic adhesives such as urea formaldehyde to the manufactured particleboards has improved the internal bond strength and dimensional stability of the panels, but at the same time, created serious gaseous emissions that are harmful to the human and environment (Hashim et al., 2011). To solve this problem, it is suggested to add biodegradable adhesives from natural sources so that the produced panels would be stronger, safer and cheaper than the use of synthetic adhesives.

Gum Arabic is one of the most ancient and best known natural gums traced back to 2650 BC (Ademoh and Abdullahi, 2009). Gum Arabic, a natural composite polysaccharide derived from exudates of *Acacia senegal* and *Acacia seyal* trees. Up to 80% of worldwide gum Arabic is produced by the *A. senegal* trees in Sudan (Dauqan and Abdullah, 2013). Gum Arabic consists of a complex mixture of arabino galactan oligosaccharide, polysaccharide and glycoprotein. It has a low reactivity, excellent adhesive properties and no interference with blended product due to its colourless, odourless, and tasteless properties (Ademoh and Abdullahi, 2009). Gum Arabic is widely used in miscellaneous applications, mainly in the food area such as in confectionery, bakery, dairy, beverages and as a microencapsulating agent. In addition, gum Arabic is being widely used for industrial purposes, such as long term stabilizer, a thickener, an emulsifier and an encapsulator in the food industry and to a lesser extent in textiles, ceramics, lithography, cosmetic and pharmaceutical application (Dauqan and Abdullah, 2013; Ibrahim et al., 2013; Wyasu and Okereke, 2012; Vanloot et al., 2012).

In this study, gum Arabic (GA) powder was used as a binder to fabricate *Rhizophora* spp. particleboards as tissue equivalent phantom material for positron emission tomography- computed tomography (PET/CT) applications. The effects of

*Rhizophora* spp. particle size and GA percentage on the physical, mechanical, and structural properties of the fabricated particleboards were evaluated. Three different particle sizes of the *Rhizophora* spp. with four GA percentage levels were utilized. The fabricated particleboards were studied in terms of density, moisture content (MC), internal bond (IB) strength, thickness swelling (TS), water absorption (WA), carbon, hydrogen, nitrogen and sulfur (CHNS) chemical composition, and microstructure analysis by field-emission scanning electron microscopy (FE-SEM). Besides, X-ray fluorescence (XRF) technique was used to measure the linear and the mass attenuation coefficients of the fabricated particleboards at effective energy range of 17.4 - 26.7 keV by determining the attenuation of  $K_{\alpha 1}$  X-ray fluorescent (XRF) photons from niobium, molybdenum, palladium, silver and tin targets. The results were compared with theoretical values of water calculated using XCOM computer program.

In addition, computed tomography (CT) scan was used to study the density distribution profile of the fabricated particleboards. The most suitable particleboard sample was used to fabricate a cylindrical head phantom to be used in PET/CT applications. The efficiency of the fabricated particleboard head phantom in measuring the surface skin dose was evaluated by comparing it with another two standard water and Perspex head phantoms of the same size and shape which were all equipped with LiF: Mg,Ti thermoluminescent detectors (TLD-100), Gafachromic XR-QA2 film pieces and the radiopharmaceutical fluorodeoxyglucose (FDG). Skin dose measurements of the three types of head phantoms were carried out under PET/CT scanning.



## 1.2 Problem Statement

Nowadays, there are a number of commercially available PET/CT test phantoms for measuring daily quality control (QC) tests, periodic, and comprehensive QC testing. However, commercial test phantoms are often considered laborious, requiring special software, or of expensive cost. For example, the primary phantom recommended for dosimetry is water phantom as water is often considered as the perfect match for soft-tissue, but it is not always practical to perform dosimetric measurements in liquid medium, thus, solid homogeneous phantoms such as polystyrene, acrylic, Perspex, and phantoms made from proprietary materials have found considerable popularity (Khan, 2010). Still, the currently available tissue and water equivalent materials have some limitations in mimicking the real tissues at low and high energy ranges due to variations in the elemental composition between the real tissue and the substitute materials (Yohannes et al., 2012).

*Rhizophora* spp. wood was reported as tissue equivalent material that matches with water and breast tissue, but it was found that raw *Rhizophora* spp. wood is not suitable to be used as a phantom material because it has the potency to warp, crack and split with time; besides to mold formation (Omar, 2007). In addition, it is not easy to control the uniformity of the density throughout the board or slab. Therefore, it was proposed that the *Rhizophora* spp. wood has to be milled into fine particles and compressed into binderless particleboards, as done by Mrashdeh, (2013).

Despite binderless particleboards showed good agreement in dosimetric properties with other standard phantom materials in radiation dosimetry, it still not very strong especially in case of internal bond strength and dimensional stability (Marashdeh,

2013). Moreover, using synthetic binders is to be avoided due to the harmful emission that threatens health and environment. Therefore, using gum Arabic in this study as a binder in particleboard manufacture might be a suitable substitute to the present available binders. Until now, no information on the properties of gum Arabic bonded particleboards made from *Rhizophora* spp. has been reported. Therefore, this investigation will be the first study utilising this biodegradable adhesive in the *Rhizophora* spp. particleboard industry.

These reasons have been the force behind the efforts to develop a new, practical, tissue equivalent head phantom from environmental friendly particleboards bonded with a fully biodegradable substance such as gum Arabic as a substitute to the synthetic resins often used in particleboard manufacture.

### **1.3 Research significance**

The significance of the research lies on the fact that it would open a new field on investigating the efficacy of utilising gum Arabic bonded *Rhizophora* spp. particleboards for dosimetric application. This would lead to a substitute source for particleboard binders which are cheap, readily available and non-chemically based. This work will also facilitate further research to extend the range of applications of new tissue equivalent materials to fabricate characterization phantoms from locally available materials to reduce the cost of purchasing commercial ones.

## **1.4 Research Objectives**

The main goal of this study is to design and evaluate a new particleboard head phantom fabricated from *Rhizophora* spp. particles bonded with gum Arabic for monitoring PET/CT systems. Few minor objectives are designed to achieve the main goal as listed below:

1. To fabricate *Rhizophora* spp. particleboards with three different particle sizes and four gum Arabic percentage levels.
2. To determine the physical, chemical, mechanical structural and attenuation properties of the fabricated particleboards and select the most suitable particleboard for manufacturing a tissue equivalent head phantom.
3. To design and fabricate *Rhizophora* spp. particleboard head phantom in cylindrical shape to mimic the human head with a simulated tumour site. TLD-100 chips and Gafchromic XR-QA2 films will be placed on the surface of each head phantom in order to measure the skin surface dose due to the PET/CT scan procedure.
4. To study the performance of the three types of head phantoms in PET/CT and compare their results.

## **1.5 Scope of Research**

In this study, gum Arabic will be used as a bio-adhesive for tissue equivalent particleboards made of the mangrove *Rhizophora* spp. wood. The particleboards which are equivalent to human tissues with appropriate CT numbers will be utilised in the design of a head phantom for PET/CT imaging. A radioactive source, thermoluminescent detectors and Gafchromic XR-QA2 films will be inserted into this

phantom to evaluate the performance of the PET/CT systems. The fabricated particleboard phantom will be evaluated in comparison with standard perspex and water head phantoms.

## **1.6 Thesis Organization**

This thesis consists of five chapters, starting with the introduction in chapter 1 where a preview of the utilisation of tissue equivalent materials for phantom fabrication will be presented. Besides, it also gives a brief description of particleboards, gum Arabic and *Rhizophora* spp., in addition to, the problem statement, research significance, research objectives, scope of the study, and thesis organization. Next, Chapter 2 contains the literature review and theory section, the chapter reviews the current research relevant to this study and introduces the background information on XRF technique, PET/CT, gum Arabic and *Rhizophora* spp. tree. In Chapter 3, the particleboard samples preparation, testing the physical, chemical, mechanical microstructure properties of the fabricated particleboards will be described. Next, the manufacturing of the head phantom will be discussed in Chapter 4. In this chapter, the discussion will focus on preparation of the gum Arabic bonded *Rhizophora* spp. particleboard head phantom and the other two Perspex and water phantoms, in addition to, the skin surface measurements. Furthermore, Chapter 5 will summarize the conclusions and give suggested recommendations for future work. Lastly, it will be followed by references, appendices and list of publications.

## CHAPTER TWO

### LITERATURE REVIEW

#### 2.1 *Rhizophora* spp. tree

*Rhizophora* spp. are common mangrove trees from the family of *Rhizophoraceae*. They are also known locally as Bakau trees. This tree is about 8 – 20 m tall and often found in parts of the mangrove forest that are flooded by normal high tide (RMBR, 2013). All *Rhizophora* species have arching stilt roots that emerge from the trunk, hence their scientific name *Rhizophora* means "root bearer" in Greek (Tan, 2001). *Rhizophora* spp. can be recognized by their characteristic prop or stilt roots at the lower part of the tree which spread over a wide area to help anchoring the tree in the unstable mangrove mud, as well as to help the plant breathe air, which is scarce in the waterlogged soil. The roots also help to exclude salt from entering the plant through a process called ultrafiltration (Yeo, 2011; Tan, 2001). Fig.2.1 shows the *Rhizophora* spp. trees.



Fig. 2.1 The mangrove *Rhizophora* spp. trees (Larut Matang) from a reserve forest in Perak, Malaysia.

*Rhizophora* spp. wood is straight, strong and extremely resistant to insects and rot, even when submerged in seawater. Hence it is used as timber for construction or repair of houses, jetties, firewood and to produce charcoal (Giesen et al., 2007). *Rhizophora* spp. woods have a high calorific value meaning that they produce more heat for the same weight. It also burns evenly and produces good quality heat, even comparable to coal. Barks of mangrove trees are rich in tannin so it is harvested for the tanning industry, toughening fishing lines and dyeing. High tannin content increases the resistance to herbivores (Giesen et al., 2007; RMBR, 2013). This tree is often planted along fish ponds to protect the bunds (Yeo, 2011). Moreover, mangrove trees are also used for the lignocellulose for the manufacture of chipboard, pulpwood, newspaper and cardboard. Many mangrove species are also exploited for their medicinal usage (Ng et al., 1999). In traditional medicine, they are used to treat angina, boils, leprosy, fever, malaria, diarrhoea, dysentery, and fungal infections (Duke and Allen, 2006).

## **2.2 Gum Arabic**

Gum Arabic (GA) is also known as Arabic gum, gum Acacia; Arabinol Powder; Gum Talha and Gum Hashab. Gum Arabic is the dried gummy exudates produced from the stems and branches of *Acacia* tree. In fact, there are more than 1000 species of *Acacia*, but only two of the *Acacia* species are significant for commercial purposes: *Acacia senegal* (L). which produces the best type of gum and provides the bulk for world trade and *Acacia seyal*, which produces a lower grade of gum (Ibrahim et al., 2013; Elnour et al., 2011). Gum from *A. senegal* (L) is considered as the best in quality

and widely used species of natural plant gums because it contains low quantities of tannins (Egadu et al., 2007). Gum Arabic which is derived from *Acacia senegal* (L) tree is known as Hashab gum in Sudan and Kordofan gum in the world (Elnour et al., 2011). Gum Arabic is commercially available in different shapes as white to orange-brown solid spheroidal tears of varying sizes with a matt surface texture, white to yellowish-white flakes, granules, powder, roller dried, or spray-dried material (Creel, 2006).

*Acacia* trees are abundant in central Sudan, central and West Africa, tropical and semitropical areas of the world (Wyasu and Okereke, 2012; Hadi et al., 2010). However, Sudan is considered as the world's largest producer followed by Nigeria, Chad, Mali and Senegal (Vanloot et al., 2012). For example, in 1966, Sudan export of the gum was between 40,000 and 50,000 tons per year and was valued at about US\$ 15–20 million (Egadu et al., 2007).

Gum Arabic is generally produced from *Acacia* tree under adverse conditions such as lack of moisture, poor nutrition, microbial attack and hot temperature. It is also produced on wounded surfaces of *Acacia* trees; thus, wounds are produced intentionally in cultivated trees by stripping barks during the dry season to stimulate the gum flow. The gum is collected by hands over a period of several weeks with an average annual yield of 250 g per tree (Wyasu and Okereke, 2012). *Acacia Senegal* tree with gum Arabic nodules appears in Fig. 2.2.



Fig. 2.2 Gum Arabic flowing from the bark of *Acacia senegal* tree (Cecil, 2005).

### 2.2.1 Chemical characteristics of gum Arabic

The chemical composition of the gum varies according to the age of trees, their location and the conditions of the soil (Valnoot et al., 2012). Basically, gum Arabic has been shown to be highly heterogeneous, complex mixture of high-molecular weight neutral or slightly acidic polysaccharides, protein and arabinoglacto protein species. It is naturally found as mixed calcium, magnesium, potassium and sodium salts of Arabic acid; a complex branched polysaccharide which on hydrolysis yields D- galactose, L- rhamnose, D-glucuronic acid and L-arabinose residues (Ibrahim et al., 2013; Wyasu and Okereke, 2012; Hadi et al., 2010). A typical analysis of *A. senegal* sugar and amino acid compositions after hydrolysis is shown in Table 2.1.



Table 2.1 Chemical composition and some properties of *Acacia senegal* gum.

| Parameter               | Value | Parameter                     | Value |
|-------------------------|-------|-------------------------------|-------|
| <b>Sugars (%):</b>      |       | <b>Amino acids (Continue)</b> |       |
| Rhamnose                | 14    | Valine                        | 0.085 |
| Arabinose               | 29    | Lysine                        | 0.075 |
| Galactose               | 36    | Alanine                       | 0.045 |
| Glucuronic acid         | 14.5  | Tyrosine                      | 0.042 |
|                         |       | Arginine                      | 0.037 |
| <b>Amino acids (%):</b> |       | Isoleucine                    | 0.031 |
| Hydroxyproline          | 0.711 | Methionine                    | 0.002 |
| Serine                  | 0.302 | Cysteine                      | -     |
| Threonine               | 0.208 | Tryptophan                    | -     |
| Proline                 | 0.180 |                               |       |
| Leucine                 | 0.198 | <b>Others:</b>                |       |
| Hestidine               | 0.166 | Nitrogen (%)                  | 0.365 |
| Aspartic acid           | 0.141 | Protein (%)                   | 2.41  |
| Glutamic acid           | 0.122 | Average molecular mass (kDa)  | 380   |
| Phenylalanine           | 0.105 |                               |       |

Source: Montenegro et al., (2012).

However, other heavy elements such as Zn, Al, Cd, Cu, Cr, Pb, and Co may also be present but in very small quantities. Gum Arabic is associated with low viscosity and absence of colour, taste and odour (Ibrahim et al., 2013). Due to its colourless, odourless, and tasteless properties, it does not interfere with the blended output. It is insoluble in organic solvents such as alcohol, but water is its main solvent. The high solubility in water makes it versatile in application, since the main solvent is cheap, readily available and non-chemically based (Ademoh and Abdullahi, 2009a). Its pH in a 25% water solution is between 4.1- 4.8 (Creel, 2006). The weak acidity makes it chemically human friendly and non corrosive to tools and equipments. The GA has a melting point of 178-210°C based on the GA grade (Ademoh and Abdullahi, 2009). The value is suitable for

particleboard manufacture since it can tolerate the high temperature and pressure applied during the particleboard preparation.

### **2.2.2 Uses of gum Arabic**

Gum Arabic has been used widely for long time ago. It was used by the Egyptians for embalming mummies, as an adhesive, and also in ink and paints for hieroglyphic inscriptions. With time, GA found its way to Europe and it started to be named "gum Arabic" since it was exported from Arabian ports (Montenegro et al., 2012). Natural gums are preferred over synthetic materials due to their non-toxicity, low cost and availability. Use of gum Arabic falls in three groups: Food, pharmaceutical and industrial.

### **2.2.3 Gum Arabic in food products**

Around 80% of the GA produced is used, worldwide, in foodstuffs; of that total, ~50% is used as a major ingredient in confectionery and the remainder is used in minor proportions (1-2%) as a food additive known as E414 (Anderson and East wood, 1989). Gum Arabic is used in foods as a stabilizer and thickener since it is non-toxic, tasteless, colourless, odourless, water-soluble, so it does not alter the food flavours. For example, GA is used as a stabilizer for frozen products such as dairy products, ice creams, and packed milk, because of its water absorbing properties. In beverages, it is used as beverage emulsion, and flavour emulsions, especially in fruit juices and cola. Due to GA

anticrystallizing property, it is a main ingredient in gummy, jellies and chocolate candies production. It is also used in the baking industry for its favourable adhesive properties in glazes and toppings (Ibrahim et al., 2013; Wyasu and Okereke, 2012).

#### **2.2.4 Medical and pharmaceutical applications of gum Arabic**

Apart from food uses, gum Arabic has wide medical applications. It was used in Arab folk medicine internally to treat inflammation of intestinal mucosa and externally to cover inflamed skin. For some time now, GA is intensively used in patients with chronic kidney failure (Ali et al., 2008). Recent reports have confirmed that GA has positive contribution on the metabolism of lipids (Tiss et al., 2001), cardiovascular (Glover et al., 2009) and gastrointestinal diseases (Wapnir et al., 2008), in addition to hypoglycaemic effects in diabetic patients (Dabaghian et al., 2012).

Moreover, dental studies revealed the inhibitory ability of GA against certain periodontal pathogenic species that cause tooth decay. Results also suggested that GA could prevent the formation of plaque and improve dental remineralisation, acting as a powerful preventive agent in the formation of caries (Onishi et al., 2008). The GA is slowly fermented by the bacterial flora of the large intestine producing short chain fatty acids. Therefore, its tolerance is excellent and can be consumed in high daily doses without intestinal complications (Montenegro et al., 2012). Gums are metabolised by the microflora in the intestines and completely degraded into their individual component sugars. In addition, enzymes available in the intestine can cleave the gums at specific

sites (Rana et al., 2011). A daily intake of 25 and 30 g of GA for 21 to 30 days reduced total cholesterol by 6 and 10.4%, respectively (Sharma 1985).

The GA is extensively used in pharmaceuticals because of its favourable properties. The GA has good adhesive and laxative properties and is, therefore, used in dental preparations. It is used as binders and disintegrants in tablets and pills. In liquid oral syrups and topical products GA is used as suspending, thickening and/or stabilizing agent (Wyasu and Okereke, 2012; Rana et al., 2011).

Gum Arabic is widely used in cosmetic production because of its non-toxicity and absence of adverse dermatological effects. It is used in lotions and protective creams to stabilize the emulsion, increase the viscosity and facilitate spreading properties (Wyasu and Okereke, 2012).

#### **2.2.5 Industrial applications of gum Arabic**

Gum Arabic is used widely in different industrial sectors such as textiles, ceramics, porcelain, and lithography due to its unique ability to emulsify highly uniform, thin liquid films. It is also used as viscosity controller in inks, pottery pigments, water colours, and wax polishes. In paints and similar formulation, gum Arabic is used as binder where it prevents hard setting of pigments (Montenegro et al., 2012; Wyasu and Okereke, 2012). Furthermore, it is a coating for papers and a key ingredient in the micro-encapsulating procedure that makes carbonless copy paper, scratch-and-sniff perfume advertisements, laundry detergents, baking mixes and aspirins, metal corrosion

inhibition, glues, fireworks, explosives, cartridge powder, insecticides and pesticides. Moreover, moisture-sensitive postage-stamp adhesives depend on it (Cecil, 2005).

#### **2.2.6 Gum Arabic as a natural adhesive**

Adhesives are defined as substances that have the ability to bind materials together by surface attachment with the capability to sustain the designed load requirement without deformation or failure (Ademoh and Abdullahi, 2009). Adhesives are generally classified as: organic adhesives, inorganic adhesives, mineral or miscellaneous adhesives depending on their source, applications, chemical composition, cost and stability.

Gum Arabic is a natural adhesive developed from *Acacia* tree by product. It found usage particularly in the manufacture of adhesives for general office purposes such as in liquid glue, postage stamps envelopes, labels, etc, because of their good affinity for water or saliva (Wyasu and Okereke, 2012). It is also used as paper gum in walling of paper. In general, natural gums are preferred over synthetic materials due to their safety, availability and low cost.

From knowledge and experiences of GA uses, it is believed that its physical and chemical properties might be compatible with those desired properties for particleboard manufacturing. Especially that the majority of wood adhesives for structural application are thermosetting phenol-formaldehyde (PF) or urea formaldehyde (UF) polymer or their derivatives. On the other hand, adhesives such as epoxy urethane and polyvinyl acetate are used as assembly for non-structural applications (Ademoh and Abdullahi,

2009). However, these synthetic adhesives are to be avoided due to their health and environmental harmful effects.

In our literature review, few studies were found interested in gum Arabic for binding applications. Ademoh and Abdullahi (2009a) investigated physical and chemical properties of Nigerian *Acacia* species to determine its viability for binding sand. They found that the Nigerian *Acacia* species exudates have great potentials for use in foundry as binders to replace imported ones since it satisfied major physiochemical properties desired of good sand binders.

On the other hand, Suleiman et al. (2013) used the natural sponge particles (rice husks) with gum Arabic and formaldehyde (top bond) for the production of particleboard. The developed particle board composites showed favourable properties compared with standard particleboards for general purpose requirements like paneling, ceilings, partitioning, etc. The microstructure, water absorptivity, and scatter index tests confirmed the possible use of sponge particles as reinforcement in the production of particleboard.

In addition, Ndububa, (2013) fabricated particleboard samples from sawdust and sieved wood shavings' specimens in a 1:1 mix proportion and combined them with gum arabic (*Acacia leguminosae*). The results showed that the sawdust and wood shavings particleboard exceeded the recommendation of the European standards for flexural and tensile strengths when the proportion of gum Arabic was between 14 and 20%. The compressive strengths at 16% resin and above exceeded the minimum acceptable value of sandcrete blocks according to Nigerian Standards Organization. The fabricated

particleboards had a maximum density of  $864.44 \text{ kg/m}^3$  suggests it as a lightweight building material. However, the water absorption capacity was far higher than the average specified value by European standards. SWSP were suggested as internal partition wall material and as internal ceiling board.

Three final year projects from Federal University of Technology, Minna- Nigeria were found dealing with gum Arabic in particleboard production. First, Sayyedi, (2006) produced particleboard from coconut shell using gum Arabic as the resin binder. It was found out that coconut shell gives quality and durable board bonded with gum Arabic. The density of particleboard was  $585.88 \times 10^3 \text{ kg/m}^3$ , and the properties of the particleboard depended on the particle size of coconut shell, quality of the resin binder, pressure and method of forming.

Second, Adegbelemi, (2010) produced particleboard from the composite of coconut and palm kernel shell using gum Arabic as the binding resin. The result of the project showed that the properties of the particle board depend on particle sizes of the shell, quality and quantity of the resin binder and method of forming. Also, the presence of palm kernel shell further strengthened and increased the density of the board. High quality and durable boards with good size requirement were produced.

Third, Usha, (2012) produced particleboards from agricultural wastes (Sawdust, Sugarcane bagasse, Melon shell and Rice husk) using Gum Arabic as a binding resin. The formed boards were subjected to compressive test, moisture content test and porosity test. The results showed that the properties of the particleboards depend on the particle sizes of the waste material, quality of the resin binder and the method of forming. The resulting particleboards were of high quality.

In this study, gum Arabic will be used as a natural adhesive for binding *Rhizophora* spp. particleboards which could be used as tissue equivalent phantom material.

### **2.3 X-ray fluorescence (XRF)**

X-Ray Fluorescence was used in this study to measure the mass attenuation coefficients of the fabricated particleboard samples because XRF is a rapid, versatile technique which offers itself to a wide variety of samples from powders to liquids. It is convenient and economical to use since it has few moving parts, low-maintenance tendency, and consumes only liquid nitrogen and electricity on a regular basis. The sample preparation for XRF is relatively simple and consumes less time and effort (Al-Eshaikh and Kadachi, 2011).

The principle of XRF can be summarized when incident high-energy photons extract a K or L inner shell electrons by the photoelectric effect and thus electron vacancies in inner shells (K, L, M, ...) are available. Then, a cascade of electron transition of outer shell electrons into these vacancies causes the emission of characteristic fluorescence radiation corresponding to the difference in energy between the atomic shells involved, as shown in Fig. 2.3.



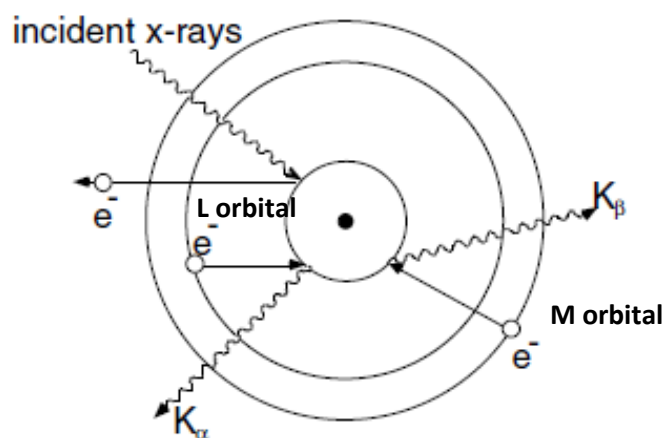


Fig.2.3 Principle of XRF radiation. Incident X-rays extract a K level electron. Either  $K_{\alpha}$  or  $K_{\beta}$  radiation is emitted, depending on whether the vacancy in the K shell is filled by an L or M electron (Riise et al., 2000).

If an L electron falls into the K orbital,  $K_{\alpha}$  radiation is emitted, while,  $K_{\beta}$  radiation is emitted if an M electron falls into the K orbital. However, within the shells there are multiple orbits of higher and lower binding energy electrons, therefore, a further designation is made as  $\alpha_1$ ,  $\alpha_2$  or  $\beta_1$ ,  $\beta_2$ , etc. to indicate transitions of electrons from these orbits into the same lower shell. The energies of K, L, and M peaks are characteristic of the particular element and independent of the matrix, so by the measurement of the wavelength or energy and the intensity of the characteristic X-ray photons emitted from the sample, the identification of the elements present and the determination of their mass or concentration becomes easy (Riise et al., 2000).

The set up of an XRF system is composed of some components which involve the radiation source, geometry of source, collimation, shield around the source, samples, detector with electronics, and data analysis software. The two major components are the excitation source to excite sample and the detector to detect the

resultant radiation. The incident radiation exciting the atoms can come from either an X-ray tube or an isotope source. The X-ray tube emits a wide spectrum of radiation and is capable of exciting a wide range of elements. Most XRF spectrometers employ an X-ray tube as the exciting energy source. Radio-isotope source, on the other hand, emits a narrow spectrum of X-rays that can only excite a narrow range of elements. X-ray isotope sources are useful when only a particular element is sought, as in certain quality control or sorting applications (Riise et al., 2000, Jenkins, 1999).

An important point is that, the source of choice for the different elements relies on the energy of the radiation source. The atoms are excited by photons having energies higher than the binding energy of the electron on the determined shells. For example, to excite  $K_{\alpha}$  line of Sn, the energy of an excited radiation must be higher than the binding energy on the Sn K shell, *i.e.*, 29.19 keV (Beckhoff et al., 2006).

After the excitation, X-ray fluorescence from the sample travels to the detector, which is cooled either electrically or with liquid nitrogen, depending on the detector type. Different types of detectors are used to measure the intensity of the emitted beam. Detectors can be classified into gas flow and scintillation. The gas flow counter is commonly used for measuring long wavelength of  $> 0.15$  nm X-rays that are typical of K spectra from elements lighter than Zn. On the other hand, the scintillation detector is utilized to analyze shorter wavelengths in the X-ray spectrum (K spectra of element from Nb to I; L spectra of Th and U). X-rays of intermediate wavelength (K spectra produced from Zn to Zr and L spectra from Ba and the rare earth elements) are generally measured by using both detectors in tandem. The intensity of the energy measured by these detectors is proportional to the abundance of the element in the sample (Wirth,

2013). In this study, Low Energy Germanium (LE-Ge) detector was used at liquid nitrogen temperatures.

The signal from the detector is then processed by the electronics and sent to the computer. A typical x-ray spectrum from an irradiated sample will display multiple peaks of different intensities. For qualitative analysis, the XRF spectrum is plotted as intensity (in counts per second for a given channel) versus energy (keV). The XRF spectra can be analyzed qualitatively and/or quantitatively using the computer software. Calibration using standards is required for reliable quantitative information (Wirth and Barth, 2013; Riise et al., 2000).

## **2.4 Positron emission tomography/computed tomography (PET/CT)**

Positron emission tomography–computed tomography (PET/CT) was employed in this study to evaluate the performance of the fabricated head phantoms. PET/CT is a new diagnostic tool that combines PET and CT scans in one device to produce a fused picture showing the anatomy and the metabolic activity of the body (Delbeke et al., 2006). This scan can be done for the whole body or a part of the body (Boellaard et al., 2010). PET/CT is used increasingly for the diagnosis, staging or restaging of tumours, as well as for the assessment of the therapy response in oncology (Picchio et al., 2012; Boellaard et al., 2010). It could also be used to diagnose a variety of diseases such as heart disease, gastrointestinal, endocrine, neurological disorders and other abnormalities within the body. Both PET and CT procedures together provide information about the position, nature of and the extent of the abnormality that offer more precise information,